Gallacher, K., Velha, P., Paul, D., Cecchi, S., Frigerio, J., Chrastina, D., and Isella, G. (2012) *1.55 μm direct bandgap electroluminescence from strained n-Ge quantum wells grown on Si substrates.* Applied Physics Letters, 101 (21). p. 211101. ISSN 0003-6951

Copyright © 2012 American Institute of Physics

A copy can be downloaded for personal non-commercial research or study, without prior permission or charge.

The content must not be changed in any way or reproduced in any format or medium without the formal permission of the copyright holder(s)

When referring to this work, full bibliographic details must be given.

http://eprints.gla.ac.uk/73084/

Deposited on: 11th December 2012

Enlighten – Research publications by members of the University of Glasgow
http://eprints.gla.ac.uk

AIP | Applied Physics Letters

1.55μm direct bandgap electroluminescence from strained n-Ge quantum wells grown on Si substrates

K. Gallacher, P. Velha, D. J. Paul, S. Cecchi, J. Frigerio et al.

Citation: Appl. Phys. Lett. **101**, 211101 (2012); doi: 10.1063/1.4767138
View online: http://dx.doi.org/10.1063/1.4767138
View Table of Contents: http://apl.aip.org/resource/1/APPLAB/v101/i21
Published by the American Institute of Physics.

Related Articles

Design and optimization of a light-emitting diode projection micro-stereolithography three-dimensional manufacturing system
Rev. Sci. Instrum. 83, 125001 (2012)

Size-dependent efficiency and efficiency droop of blue InGaN micro-light emitting diodes
Appl. Phys. Lett. 101, 231110 (2012)

A bright cadmium-free, hybrid organic/quantum dot white light-emitting diode
Appl. Phys. Lett. 101, 233110 (2012)

Interplay of polarization fields and Auger recombination in the efficiency droop of nitride light-emitting diodes
Appl. Phys. Lett. 101, 231107 (2012)

Precise relationship between voltage and frequency at the appearance of negative capacitance in InGaN diodes
Appl. Phys. Lett. 101, 233506 (2012)

Additional information on Appl. Phys. Lett.

Journal Homepage: http://apl.aip.org/
Journal Information: http://apl.aip.org/about/about_the_journal
Top downloads: http://apl.aip.org/features/most_downloaded
Information for Authors: http://apl.aip.org/authors

ADVERTISEMENT

AIP | Applied Physics Letters
EXPLORE WHAT'S NEW IN APL
SUBMIT YOUR PAPER NOW!
SURFACES AND INTERFACES
Focusing on physical, chemical, biological, structural, optical, magnetic and electrical properties of surfaces and interfaces, and more...
ENERGY CONVERSION AND STORAGE
Focusing on all aspects of static and dynamic energy conversion, energy storage, photovoltaics, solar fuels, batteries, capacitors, thermoelectrics, and more...

Downloaded 11 Dec 2012 to 130.209.6.41. Redistribution subject to AIP license or copyright; see http://apl.aip.org/about/rights_and_permissions

1.55 μm direct bandgap electroluminescence from strained n-Ge quantum wells grown on Si substrates

K. Gallacher,[1] P. Velha,[1] D. J. Paul,[1,a)] S. Cecchi,[2] J. Frigerio,[2] D. Chrastina,[2] and G. Isella[2]
[1]*University of Glasgow, School of Engineering, Rankine Building, Oakfield Avenue, Glasgow G12 8LT, United Kingdom*
[2]*L-NESS, Dipartimento di Fisica del Politecnico di Milano, Polo Territoriale di Como, Via Anzani 42, I-22100 Como, Italy*

(Received 15 May 2012; accepted 29 October 2012; published online 19 November 2012)

Electroluminescence from strained n-Ge quantum well light emitting diodes grown on a silicon substrate are demonstrated at room temperature. Electroluminescence characterisation demonstrates two peaks around 1.55 μm and 1.8 μm, which correspond to recombination between the direct and indirect transitions, respectively. The emission wavelength can be tuned by around 4% through changing the current density through the device. The devices have potential applications in the fields of optical interconnects, gas sensing, and healthcare. © *2012 American Institute of Physics*. [http://dx.doi.org/10.1063/1.4767138]

There is presently increased interest in using Ge as an active material on Si substrates to realise light emitting diodes (LEDs), lasers, and photodetectors that can either be integrated with complementary metal-oxide semiconductor electronics or provide added functions for More-than-Moore applications.[1] The potential applications include fibre-to-the-home, chip-to-chip optical interconnects in addition to longer wavelength healthcare and pollution monitoring applications.[2] Previous works have demonstrated electroluminescence from Ge p-i-n structures or other configurations grown on top of standard Si wafers.[3–7] Electroluminescence has also been demonstrated from Ge quantum well devices but so far the emission has been at wavelengths below 1.45 μm (Ref. 7) which is too low for the important 1.55 μm for telecoms. Longer wavelengths are also desirable for pollution monitoring and bio-sensing applications. The higher concentration of carriers in a two dimensional (2D) quantum well system compared to bulk three dimensional devices should ultimately allow higher efficiencies with lower thresholds ideal for all applications. Tensile-strained Ge QWs have demonstrated direct-gap transitions.[8,9] In this work, electroluminescence from strained 10 period n-Ge multiple quantum well (MQW) LEDs grown directly on a silicon wafer is presented which produces electroluminescence at the important 1.55 μm wavelength at room temperature (298 K).

The material was grown on a p-Si (100) substrate with a resistivity of 1 Ωcm. The substrate was degassed at 316 °C for 10 min before loading into a low-energy plasma-enhanced chemical vapour deposition (LEPECVD) chamber.[7,10] The heterolayer design is shown in Fig. 1. A 2.1 μm two step buffer with first a 600 nm relaxed layer of $Si_{0.61}Ge_{0.39}$ was grown followed by 1.5 μm relaxed $Si_{0.048}Ge_{0.952}$. Next 100 nm of p-$Si_{0.048}Ge_{0.952}$ ($N_A = 3 \times 10^{18}$ cm^{-3} doped from B_2H_6) was grown as required for the bottom Ohmic contact. The Ge concentrations (and quantum well thicknesses) for all heterolayers was measured after growth using x-ray diffraction (XRD). A 30 nm spacer of $Si_{0.048}Ge_{0.952}$ ($N_A = 5 \times 10^{17}$ cm^{-3}) was grown before the active quantum well region. The active region consists of 10 periods of strained 11.2 nm n-Ge quantum wells ($N_D = 1 \times 10^{19}$ cm^{-3} doped with PH_3) and 8.5 nm $Si_{0.014}Ge_{0.986}$ barriers. A final cap of 10 nm of $Si_{0.048}Ge_{0.952}$ followed by 3 nm of Si was grown to produce a Schottky top contact that would allow hot electron injection into the Γ-valley with the aim of producing more efficient direct recombination. Whilst the PH_3 was only switched on during the growth of the quantum wells, due to segregation effects, all the heterolayers grown after the first quantum well will be doped with significant fractions of the n-type doping level.[11] For this strain relaxed buffer Ge concentration, the calculated Matthews and Blakeslee critical thickness is 283 nm.[12]

The band structure was calculated using a self-consistent Poisson-Schrödinger solver with the deformation potentials from Reference 13 and the results for a single

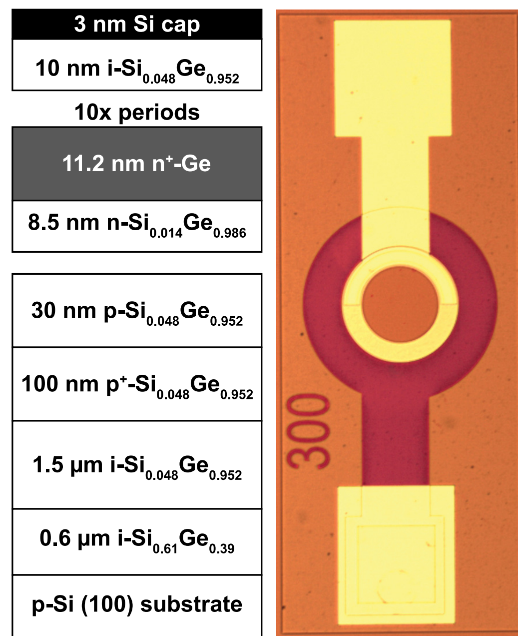

FIG. 1. The heterolayer design for the device. Right: Optical microscope picture of a completed LED.

a)Douglas.Paul@glasgow.ac.uk.

Downloaded 11 Dec 2012 to 130.209.6.41. Redistribution subject to AIP license or copyright; see http://apl.aip.org/about/rights_and_permissions

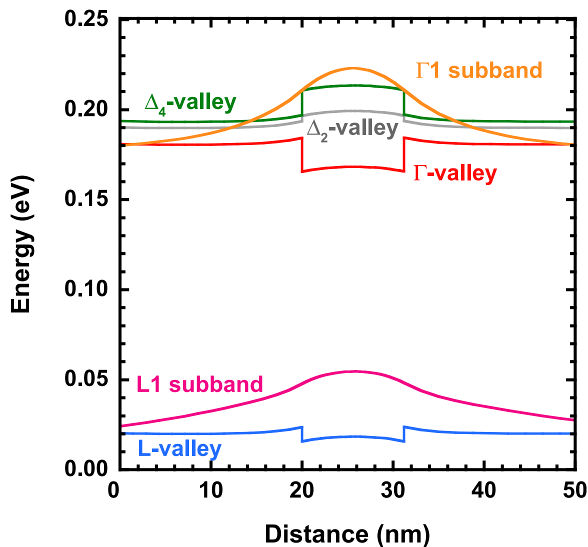

FIG. 2. The conduction bands for a single quantum well in the device as calculated by self-consistent Poisson-Schrödinger solver at 300 K. The confined subband states for the L- and Γ-valleys are also plotted.

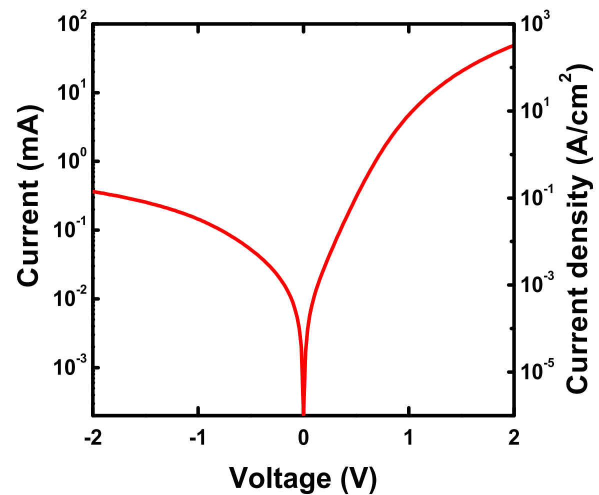

FIG. 3. The current-voltage characteristics of the device at room temperature.

quantum well are shown in Fig. 2. An 8-band **k.p** model was used for the hole bands and the Γ-valley whilst a 1 band tool was used to find the L- and Δ-valley bands and subband states. The present thin buffer resulted in a tensile strain of 0.13% as measured by XRD after the sample was cooled to room temperature and the modelling of the bands and subband states has taken account of this strain.[13] For both the L- and Γ-valleys, only a single subband for each valley is confined in the quantum well. The L-valley subband state is very weakly confined in the quantum well due to the small conduction band discontinuity of only 8 meV. At room temperature, confinement due to the L-valley quantum well is unlikely to be observed. The Γ-valley is below both Δ-valley bands due to the tensile strain in the substrate. The Γ-valley quantum well has a discontinuity of 19 meV with a single confined state that due to the low effective mass of $0.038m_0$ (where m_0 is the free electron mass), the subband states in each quantum well overlap to form a miniband with width calculated to be 8.4 meV. Modelling of the valence band demonstrated that the ground state is the heavy-hole (HH) and the lowest subband is the HH1. The tensile strain is therefore not great enough to move the LH band above the HH band. The calculated lowest direct transition is Γ1 to HH1 at 0.817 eV (1.52 μm wavelength) and the indirect L1 subband to HH1 is 0.663 eV (1.89 μm).

Cylindrical mesas ranging from 10 μm to 500 μm in diameter (see Fig. 1) were defined by a Vistec VB6 electron beam lithography tool with hydrogen silsesquioxane (HSQ) resist and then etched down anisotropically using a fluorine based chemistry in an inductively coupled plasma reactive ion etch tool. 50 nm of Ni was deposited by electron-beam evaporation for the bottom contact and this was patterned by lift-off and subsequently annealed at 340 °C for 30 s in a rapid thermal annealer (RTA).[14] The process provides bottom Ohmic contacts with measured specific contact resistivities of 4×10^{-8} Ωcm^2. An unannealed top contact of 10 nm of Ti followed by 50 nm of Al was deposited to produce a Schottky top contact which could inject carriers above the conduction band edge. The whole structure was passivated with Si_3N_4 and via holes were etched to allow interconnects to the contacts. Bond pads of 600 nm of Al were deposited and finally, the device was wire bonded to a chip carrier in order to connect the LED to an external power supply for characterisation. All results in this publication were from devices of 300 μm diameter measured at room temperature.

The current-voltage characteristics are shown in Fig. 3. Larger currents flow when the device is forward biased with electrons being injected into the conduction band from the Schottky top contact. The dark current is comparable to some of the best reported from Ge on Si photodetectors.[15] Both the photoluminescence (PL) and electroluminescence from the LED were measured using a Bruker Vertex 70v FTIR system. The FTIR system uses a calcium fluoride beamsplitter and a room temperature extended InGaAs detector, which can detect radiation between 0.8 and 2.5 μm. All measurements were undertaken in surface emission geometry which corresponds to xy-polarization (TE polarization). The selection rules for such polarization allow the following transitions:[13] Γ1 to HH1, L1 to HH1, Γ1 to LH1, and L1 to LH1. Fig. 4 shows the PL for 580 nm CW excitation. Comparison with the band structure modelling of Fig. 1 indicates that the sharper peak just above 1.5 μm is the Γ-valley to HH1 transition and the broader 1.8 μm peak is the L-valley to HH1 indirect transition. Above 2 μm is blackbody emission under CW illumination. Fig. 5 shows the electroluminescence as a function of current under CW conditions at room temperature. As the current is increased, the direct bandgap (Γ-valley to HH1) electroluminescence increases compared to the indirect (L-valley to HH1) transitions. Also the blackbody contribution demonstrates significant increases as the current is increased especially beyond the 2 μm wavelength.

Fig. 6 demonstrates the total electroluminescence-current (LI) data from the LEDs. Below 210 A/cm^2, the gradient of the LI curve is below 1 whilst above this point, the gradient increases to 1.5 and it is clear that blackbody emission from Joule heating of the sample starts to become more significant in the measured electroluminescence power. Previous publications have indicated that heating can help excite

Downloaded 11 Dec 2012 to 130.209.6.41. Redistribution subject to AIP license or copyright; see http://apl.aip.org/about/rights_and_permissions

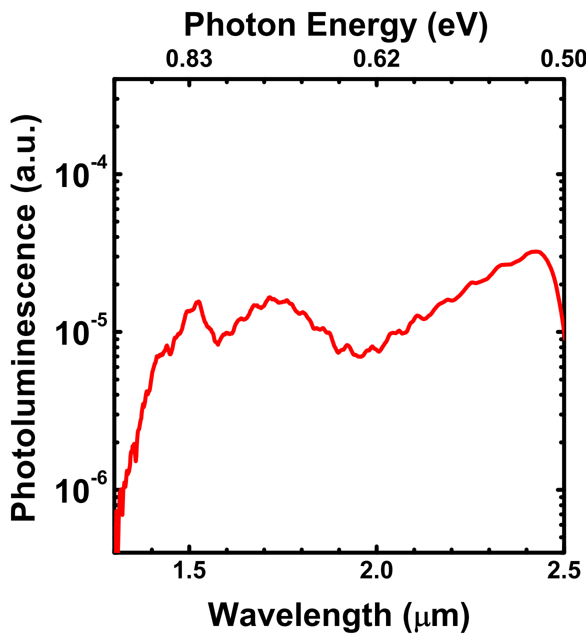

FIG. 4. The photoluminescence of the device at room temperature using a 580 nm pump source.

carriers from the L-valley to the Γ-valley and increase the electroluminescence efficiency and output power.[7,16,17] A similar effect is observed in the present devices as the ratio of the emission from the direct bandgap compared to the indirect bandgap emission increases with increasing current density but the use of the longer wavelength detector in this work also demonstrates the resulting strong spectral contribution of the blackbody emission at longer wavelengths.

Fig. 7 shows the shift in the direct bandgap recombination peak as a function of current density. As the current density is increased to 420 A/cm^2, the emission wavelength is increased by around 4% as shown in Fig. 7. The clear red-shift in the direct bandgap electroluminescence recombination peak as a function of increasing current demonstrates the Joule heating of the device with the resultant reduction in the direct bandgap (the indirect bandgap is also reduced by the heating). The bandgap dependence of Ge was modelled by Varshni[18] and the expected variation is inverse linearly proportional to the temperature when the semiconductor is well above the Debye temperature of 374 K for Ge. Curve fits to the blackbody part of the spectra in Fig. 5 indicate that the electron temperature is above 400 K for current densities of 50 A/cm^2 and above thereby indicating that the bandgap is decreasing with a linear variation of temperature. As Joule heating in semiconductors results in a near linear temperature rise with current density, the linear variation of wavelength with current density in Fig. 7 therefore agrees with the Varshni model for the bandgap for temperatures above the Debye temperature.[18] At 300 A/cm^2, the direct recombination electroluminescence is at the important 1.55 μm wavelength for telecoms applications.

To date, the majority of Ge quantum well devices have only demonstrated PL emission characterisation through

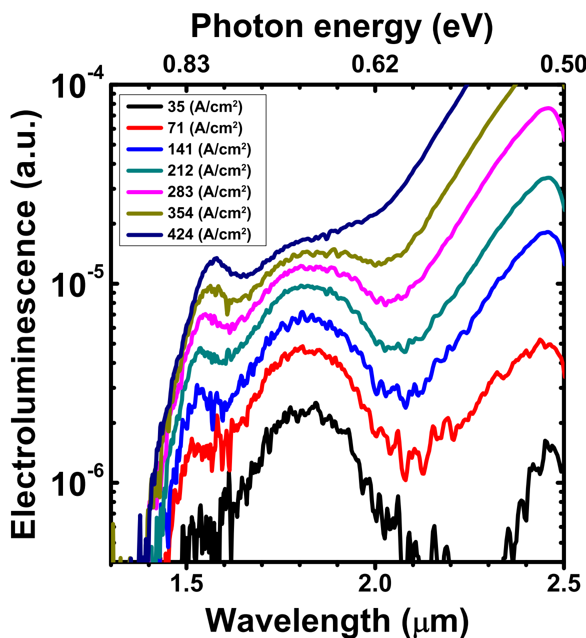

FIG. 5. The electroluminescence of the device at room temperature as a function of CW excitation currents.

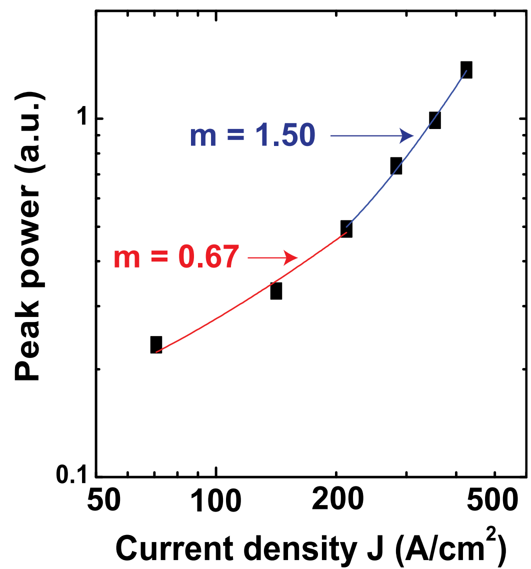

FIG. 6. The electroluminescence versus current density plot of the device at room temperature.

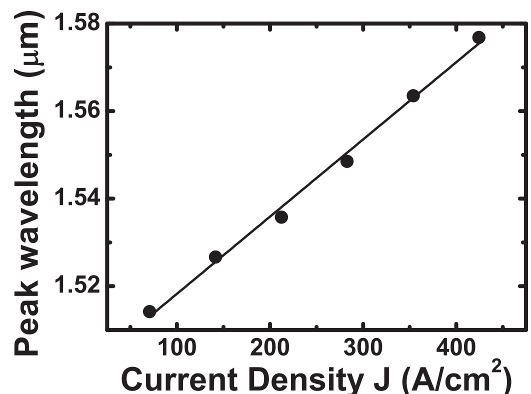

FIG. 7. The central position of the direct bandgap (Γ-valley to HH) electroluminescent peak as a function of current density at room temperature. The line is a linear fit to the data.

Downloaded 11 Dec 2012 to 130.209.6.41. Redistribution subject to AIP license or copyright; see http://apl.aip.org/about/rights_and_permissions

optical pumping. Most electroluminescence has been demonstrated with bulk n-Ge apart from a single result with emission below 1.45 μm wavelength.[7] The present n-Ge quantum well devices have a narrow direct recombination peak ($\sim$80 nm full width half maximum) followed by the drop in electroluminescence to near zero levels at higher energies (Fig. 5). This can be explained by the sharp two 2D density of states which results in only the Γ-valley to HH1 and L-valley to HH1 recombination transitions being observed under electroluminescence, unlike the bulk Ge devices. Such 2D radiative transitions are ultimately expected to produce higher gain and lower thresholds if a laser can be produced.[3] The quantum well structures also provide a natural design for confining (and guiding) the mode and therefore the expectation is that this approach is interesting to produce practical Ge electroluminescent LEDs and lasers on silicon substrates.

The direct bandgap Γ-valley to HH1 electroluminescence from n-Ge quantum wells on silicon substrates has been demonstrated from LEDs at the important 1.55 μm wavelength with CW operation. The emission wavelength of the devices can be tuned by approximately 4% through changing the current density. At higher wavelengths, the indirect L-valley to HH1 transition is observed before blackbody emission is observed. Such devices may be integrable into Si photonic circuits, and lasing may be feasible with such designs when fabricated into a suitable cavity.

[1]J. Liu, X. Sun, R. Camacho-Aguilera, L. C. Kimerling, and J. Michel, Opt. Lett. **35**, 679 (2010).
[2]D. J. Paul, Electron. Lett. **45**, 582 (2009).
[3]J. Liu, X. Sun, L. C. Kimerling, and J. Michel, Opt. Lett. **34**, 1738 (2009).
[4]X. Sun, J. Liu, L. C. Kimerling, and J. Michel, Opt. Lett. **34**, 1198 (2009).
[5]M. de Kersauson, R. Jakomin, M. E. Kurdi, G. Beaudoin, N. Zerounian, F. Aniel, S. Sauvage, I. Sagnes, and P. Boucaud, J. Appl. Phys. **108**, 023105 (2010).
[6]D. Nam, D. Sukhdeo, S.-L. Cheng, A. Roy, K. C.-Y. Huang, M. Brongersma, Y. Nishi, and K. Saraswat, Appl. Phys. Lett. **100**, 131112 (2012).
[7]P. Chaisakul, D. Marris-Morini, G. Isella, D. Chrastina, N. Izard, X. L. Roux, S. Edmond, J.-R. Coudevylle, and L. Vivien, Appl. Phys. Lett. **99**, 141106 (2011).
[8]Y. Chen, C. Li, H. Lai, and S. Chen, Nanotechnology **21**, 115207 (2010).
[9]L. Carroll, F. Imbert, H. Sigg, M. Süess, E. Müller, M. Virgilio, G. Pizzi, P. Rossbach, D. Chrastina, and G. Isella, Appl. Phys. Lett. **99**, 031907 (2011).
[10]E. Gatti, E. Grilli, M. Guzzi, D. Chrastina, G. Isella, and H. von Känel, Appl. Phys. Lett. **98**, 031106 (2011).
[11]Z. Suet, D. J. Paul, J. Zhang, and S. G. Turner, Appl. Phys. Lett. **90**, 203501 (2007).
[12]D. J. Paul, Laser Photon. Rev. **4**, 610 (2010).
[13]D. J. Paul, Phys. Rev. B **77**, 155323 (2008).
[14]K. Gallacher, P. Velha, D. J. Paul, I. MacLaren, M. Myronov, and D. R. Leadley, Appl. Phys. Lett. **100**, 022113 (2012).
[15]J. Osmond, G. Isella, D. Chrastina, R. Kaufmann, M. Acciarri, and H. von Känel, Appl. Phys. Lett. **94**, 201106 (2009).
[16]S.-L. Cheng, J. Lu, G. Shambat, H.-Y. Yu, K. Saraswat, J. Vuckovic, and Y. Nishi, Opt. Exp. **17**, 10019 (2009).
[17]P. H. Wu, D. Dumcenco, Y. S. Huang, H. P. Hsu, C. H. Lai, T. Y. Lin, D. Chrastina, G. Isella, E. Gatti, and K. K. Tiong, Appl. Phys. Lett. **100**, 141905 (2012).
[18]Y. P. Varshni, Physica **34**, 149 (1967).

Downloaded 11 Dec 2012 to 130.209.6.41. Redistribution subject to AIP license or copyright; see http://apl.aip.org/about/rights_and_permissions